

# Wnt-14 Plays a Pivotal Role in Inducing Synovial Joint Formation in the Developing Appendicular Skeleton

Christine Hartmann and Clifford J. Tabin\*

Department of Genetics  
Harvard Medical School  
Boston, Massachusetts 02115

## Summary

The long bones of the vertebrate appendicular skeleton arise from initially continuous condensations of mesenchymal cells that subsequently segment and cavitate to form discrete elements separated by synovial joints. Little is known, however, about the molecular mechanisms of joint formation. We present evidence that *Wnt-14* plays a central role in initiating synovial joint formation in the chick limb. *Wnt-14* is expressed in joint-forming regions prior to the segmentation of the cartilage elements, and local misexpression of *Wnt-14* induces morphological and molecular changes characteristic of the first steps of joint formation. Induction of an ectopic joint-like region by *Wnt-14* suppresses the formation of the immediately adjacent endogenous joint, potentially providing insight into the spacing of joints.

## Introduction

Key to both relative size and articulation of the forming appendicular skeleton is the process of segmentation where initially continuous precartilagenous condensations are separated into discrete elements. The initial patterning of the appendicular skeleton is controlled by molecular signals establishing spatial coordinates in the early limb bud prior to the differentiation of the mesenchyme (for reviews, see Wolpert, 1990; Izpisua-Belmonte and Duboule, 1992; Hinchliffe, 1994; Johnson et al., 1994; Tickle, 1995; Zakany and Duboule, 1999). Based on the early positional information, a mesenchymal condensation forms first in the proximal region of the limb, forming the anlagen of the humerus (or femur) and proceeds distally, branching as it extends to form the ulna and radius (or fibula and tibia). The distal portion of the ulna (fibula) further branches and subsequently segments to form the posterior proximal carpal (tarsal) element, the ulnare (fibulare), and the distal carpal (tarsal) element, as well as the digital rays of digits IV–II. Significantly, these early branched, prechondrogenic condensations within each limb appear spatially continuous (as revealed by staining with Alcian blue, a dye specifically reacting with the extracellular matrix [ECM] components of the chondrocytes), and only subsequently segment into individual skeletal elements. Thus, although a few elements form from independent condensations, most of the limb skeleton is thought to arise by branching and segmentation of preexisting prechondrogenic elements (Hinchliffe and Johnson, 1980; Shubin and Alberch, 1986; Oster et al., 1988).

Morphologically, development of most articulations begins with the formation of regions with higher cell density at the site of the future joints, called interzones. Cells of the interzones appear flattened, and lose some of the characteristics of early prechondrogenic cells, including the downregulation of certain ECM components (Craig et al., 1987), reflected in a gradual loss of Alcian blue staining. The interzone in the chick develops into a three-layered structure comprised of a region of decreased cell density (called the central intermediate lamina) flanked by two areas of higher cell density that ultimately form the articular cartilage (Mitrovic, 1977). Cells in the central intermediate lamina are progressively lost through apoptosis (Ballard and Holt, 1968; Mitrovic, 1977; Mori et al., 1995; Nalin et al., 1995; Kimura and Shiota, 1996), leading to the formation of the joint cavity (a process referred to as cavitation). Previous studies have suggested that the synthesis of hyaluronan, its interaction with specific receptors such as CD44, and movement of the limbs (reviewed by Pitsillides, 1999), are necessary for cavitation of the joint. Meanwhile, the joint capsule and tendon attachments to the adjacent muscles form from surrounding mesenchymal cells. The mature joint is comprised of the two opposing fibrous articular cartilage surfaces of the adjacent bones separated from each other by a liquid-filled joint cavity, and surrounded by a joint capsule composed of fibrous connective tissue, locally strengthened by ligaments and lined on the inside by the synovial membrane.

Despite their importance, the molecular processes regulating formation and patterning of the skeletal elements are only beginning to be elucidated (Hall and Miyake, 1995, 2000; reviewed by Francis-West et al., 1999b) and significantly, there have been no genes reported that have the ability to initiate the process of joint formation. Nonetheless, a few signals are known that appear to be required for some aspects of segmentation. In particular, several members of the growth and differentiation factor (GDF) subfamily of TGF $\beta$  molecules, which are closely related to the bone morphogenic proteins (BMPs), are expressed in forming joints (Storm and Kingsley, 1996, 1999; Wolfman et al., 1997; Francis-West et al., 1999a; Merino et al., 1999), and one of these, *Gdf5*, is mutated in the brachypodism (*bp*) mouse mutant (Storm et al., 1994), which is characterized by a segmentation defect of the phalangeal skeletal elements (Landauer, 1952; Grüneberg and Lee, 1973; Storm and Kingsley, 1996). Mutations in *CDMP1*, the human *Gdf5* homolog, are likewise associated with skeletal abnormalities, including defects in joint development (Thomas et al., 1996, 1997; Polinkovsky et al., 1997). However, in spite of the requirement for this factor in the formation of specific joints, gain-of-function experiments with *Gdf5* in both chick and mouse result in ectopic growth of cartilage but do not lead to morphological or molecular changes characteristic of the formation of a new joint (Francis-West et al., 1999a; Merino et al., 1999; Storm and Kingsley, 1999).

\*To whom correspondence should be addressed (e-mail: tabin@rascal.med.harvard.edu).

A number of *Wnt* genes have been implicated in various aspects of chondrogenesis (Zakany and Duboule, 1993; Rudnicki and Brown, 1997; Kawakami et al., 1999; Yamaguchi et al., 1999; Hartmann and Tabin, 2000). One of these, *Wnt-4*, has been reported to be expressed in the developing joint regions (Kawakami et al., 1999; Hartmann and Tabin, 2000). However, further analysis revealed that *Wnt-4* does not play a role in joint development, but acts on adjacent cartilage to promote chondrocyte maturation (Hartmann and Tabin, 2000). Here, we report that another member of this gene family, *Wnt-14*, is also expressed in developing joints. In contrast to previously reported signaling molecules expressed in joint forming regions, *Wnt-14* misexpression induces morphological and molecular signs of joint formation, indicating that *Wnt-14* plays a crucial role in the initiation of synovial joint development.

## Results

### Expression of *Wnt-14* in the Developing Chick Autopod

In a comprehensive screen for *Wnt* genes expressed during skeletogenesis in the chick, we isolated a probe for *Wnt-14* based on the previously published sequence (Bergstein et al., 1997). Preliminary analysis indicated that *Wnt-14* was expressed within developing joints. We compared the expression of *Wnt-14* to that of *Gdf5*, which has previously been shown to be expressed in the developing joint (Figure 1). At day 5 of development, *Wnt-14* is expressed in a transverse stripe in the presumptive joint region of the future metatarsophalangeal joints of digits II-IV (Figure 1A), as well as in the interdigital nonchondrogenic mesenchyme (Figure 1A'). *Gdf5* at this stage is expressed in a similar pattern (Figures 1B and 1B'). Two days later, *Wnt-14* continues to be expressed in the mesenchyme surrounding the cartilage elements, as well as in a bipartite stripe within the joint region (Figure 1C). At the same stage, *Gdf5* is present at high levels in the joint region, and continues to be expressed in the mesenchyme surrounding the digit elements, but in a more restricted domain that is limited to the perichondrium (Figure 1D; Francis-West et al., 1999a). At later stages, *Wnt-14* continues to be expressed in joints and in the nonchondrogenic mesenchyme surrounding the phalangeal elements (Figure 1E), while *Gdf5* at these stages is expressed exclusively in a horseshoe-like pattern at the joints (Figure 1F). Note that at all of these stages, the mesenchymal expression of *Wnt-14* is limited to soft tissue next to the skeletal elements (e.g., white arrow in Figure 1E) and is excluded from the perichondrium (e.g., stained dark blue, see red arrowhead in Figure 1E). Thus, the only expression of *Wnt-14* in the chondrogenic region is in the forming joint. *Wnt-14* may have a distinct role in the soft tissue adjacent to the skeletal elements in differentiation of tendons or other soft tissue derived structures. Finally, in fully-developed joints of both the elbow and the knee (days 12 and 15, respectively), we detect *Wnt-14* expression in portions of the fibrous connective tissue of the joint capsules, as well as in the synovial membrane lining the inside of the joint capsule (Figures 1G-1I). In addition, *Wnt-14* expression at these later stages is seen in

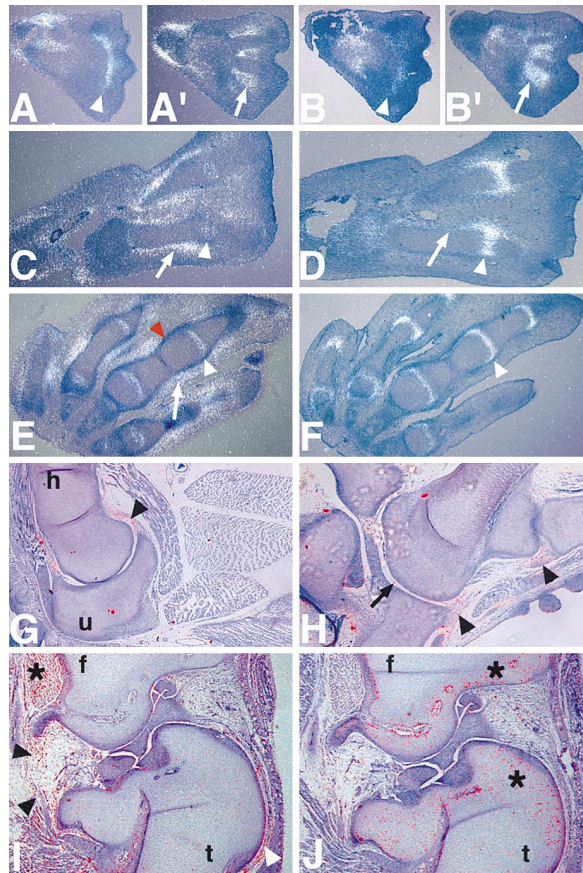


Figure 1. *Wnt-14* Is Expressed in a Pattern Similar to the Joint Marker *Gdf5*

Alternate 5  $\mu$ m sections through the autopod region of legs (A-F, I, and J) and wings (G and H) of chick embryos from day 6-15 hybridized with radiolabeled antisense riboprobes for *Wnt-14* (A, A', C, E, and G-I) and *Gdf5* (B, B', D, F, and J).

(A) *Wnt-14* expression at the future metatarsophalangeal (MTP) joint regions of digits II-IV (arrowhead) at stage 27 and (A') in the interdigital regions (arrow).

(B) *Gdf5* expression in the MTP joint region at stage 27 (arrowhead) and (B') in the interdigital regions (arrow). *Wnt-14* expression in the joints (arrowhead) and interdigital mesenchyme at stage 29 (C) and at stage 33 (F). *Gdf5* expression in the joints (arrowhead) and in the perichondrium (arrow) at stage 29 (D) and at stage 33 (F).

(G and H) Sections through the elbow and carpal regions of a day 12 wing, showing *Wnt-14* expression (signal in red) in joint capsules (arrowheads in G and H) and in protrusions of the synovial membrane into the joint cavity (arrow in H).

(I-J) Alternate sections through the knee of a day 15 chick embryo. (I) *Wnt-14* expression (signal in red) in structures of the joint capsule (black arrowhead), in the synovial membrane (white arrowhead), and in muscles (asterisk). (J) *Gdf5* expression (signal in red) in the fibroarticular cartilage of the knee joint (asterisks). All sections are orientated proximal to the left. h, humerus; u, ulna; f, femur; t, tibia.

both tendons and muscles (Figure 1I and data not shown). In contrast, *Gdf5* expression at these stages is restricted to the fibroarticular cartilage of the joint (Figure 1J).

### *Wnt-14* Misexpression Induces Morphological Changes Consistent with Joint Formation

To evaluate a potential role for *Wnt-14* in joint formation, we used a retroviral vector to misexpress it in the poste-

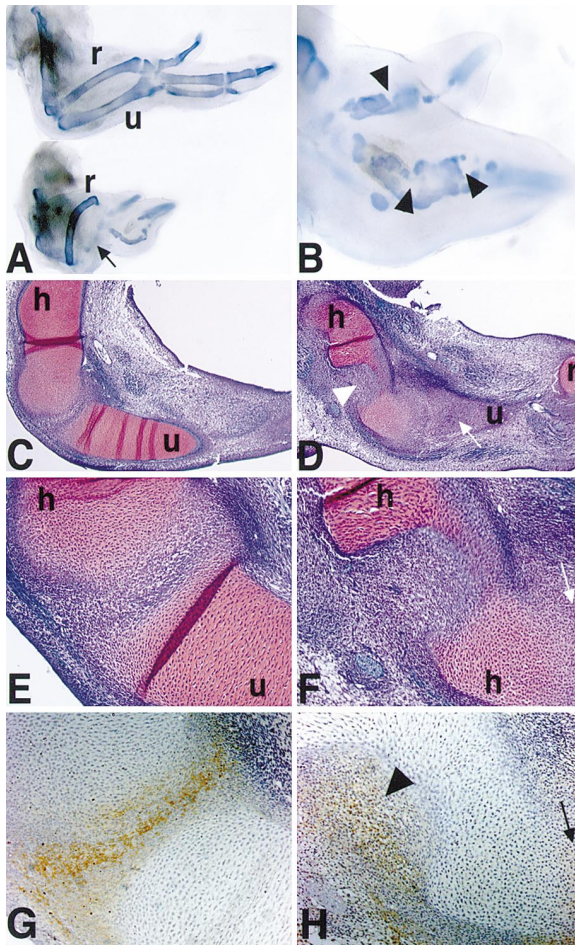


Figure 2. Morphological and Histological Changes in the Skeletal Elements Induced by Retroviral Misexpression of *Wnt-14*

(A–B) Alcian blue staining of skeletal elements at day 9.5 of development. (A) Wing pair showing the normal skeletal pattern of the left uninjected wing (upper wing) and the changes in the skeletal elements induced by *Wnt-14* viral injections into the posterior region of the limb on day 3.5 (lower wing), where the ulna is smaller and weakly stained (arrow). (B) High magnification of the autopod of a *Wnt-14*-infected wing, showing multiple gaps in the digital elements (arrowheads).

(C–H) Histological analysis on alternate 6  $\mu\text{m}$  sections through an uninfected (C, E, and G) and a *Wnt-14*-infected wing (D, F, and H) at day 7. (C–F) Weigert-SafraninO staining of sections through a wing at day 7; chondromucin-rich ECM of the chondrocytes is stained in red, nuclei are in black, and other cells are stained in purple. (C) Contralateral uninfected wing. (D) Affected ulna (arrow) and indentation in the humerus (arrowhead) in a *Wnt-14*-infected wing. (E) High magnification of a normal elbow joint. (F) High magnification of the indentation in the humerus shown in (D); the arrow is indicating the elbow joint. (G–H) Immunohistochemical staining for collagen type III (Col III; shown in brown). (G) Normal elbow joint. (H) Col III positive cells within the indentation of the humerus (arrowhead), the arrow is indicating the elbow joint. All limbs are orientated proximal to the left, anterior up. h, humerus; u, ulna; r, radius.

rior region of developing chick limbs. Infected limbs show severe alterations of the skeletal pattern (Figure 2), unlike those seen previously in similar misexpression studies using other *Wnt* genes (Rudnicki and Brown, 1997; Kawakami et al., 1999; Hartmann and Tabin, 2000). In particular, the phenotypic effects assayed by Alcian

blue staining ranged from an almost complete absence of cartilage elements in heavily infected regions (ulna, Figure 2A) to gaps in the cartilage matrix in partially infected elements (digits, Figures 2A and 2B). Histological analysis of such limbs revealed that in the heavily infected regions, which stained weakly with Alcian blue, the prechondrogenic condensations had formed but did not show any signs of further chondrogenic differentiation (compare Figure 2D with 2C).

The morphology of *Wnt-14*-infected chondroblasts is very similar to that of cells in the normal joint interzone (compare Figure 2F to 2E). The cells are densely packed and their ECM stains only weakly with SafraninO, indicating that the ECM of these cells has a lower chondromucin content, similar to cells found in the normal joint interzone. In addition, immunohistochemical stainings revealed that the infected cells express collagen type III (arrowhead, Figure 2H), a characteristic matrix component of developing joints (Figure 2G; Ros et al., 1995). Thus, by both morphological and histological criteria, *Wnt-14* is able to induce changes in the developing skeletal elements that are consistent with the initiation of ectopic joint formation.

#### Wnt-14 Arrests and Reverses Chondrogenic Differentiation In Vitro

During the normal process of joint formation, mesenchymal condensations lose Alcian blue staining in joint-forming regions as cells exit the chondrogenic pathway. Similarly, when we misexpressed *Wnt-14* in vivo, the developing skeletal elements displayed gaps in Alcian blue staining in the infected regions (Figures 2A and 2B). To verify that *Wnt-14* is capable of reverting Alcian blue-positive condensations to an Alcian blue-negative state, micromass cultures (MMC) were made from mesenchymal cells of stage 22–23 limb buds, just prior to the initiation of chondrogenesis. Over the normal course of a 4 day culture period, such MMCs first condense to form a field of prechondrogenic nodules which can be identified by light Alcian blue staining, and subsequently differentiate into nodules which are strongly Alcian blue positive (Ahrens et al., 1977).

Infection of limb mesenchymal cells with *Wnt-14* virus at culture day 0 completely inhibited the formation of Alcian blue-positive cartilage nodules, assayed on day 4 (Figure 3D). Immunohistochemical peanut-agglutinin staining revealed that the mesenchyme in *Wnt-14*-infected cultures condenses to form precartilaginous aggregates (assayed on day 3, Figure 3E) similar to control cultures (data not shown), but these aggregates do not differentiate into cartilage nodules. In contrast, control cultures infected with retroviruses expressing human *alkaline phosphatase* (*AP*) consisted by day 4 of a lawn of closely packed cartilage nodules that stained strongly for Alcian blue (Figure 3A). Next, we asked whether *Wnt-14* could reverse the light Alcian blue staining that is characteristic of initial mesenchymal condensations both in vivo and in vitro. After 2 days in culture, mesenchymal cells typically form nodules which stain lightly with Alcian blue (Figure 3F). Parallel sets of MMCs were cultured from day 2 onwards in the presence of media containing either *AP* (control), or *Wnt-14* viral particles (Figures 3G and 3J). After two more days, the control

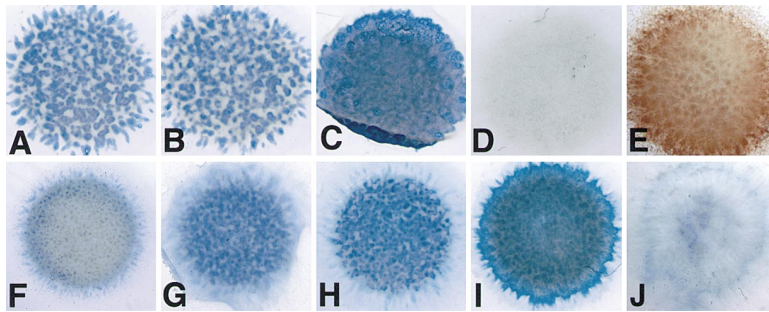


Figure 3. Alcian Blue Staining of Micromass Cultures (MMC) Showing that Wnt-14 Arrests and Reverses Chondrocyte Differentiation In Vitro

(A–D) Distribution of Alcian blue–positive cartilage nodules in MMC at day 4 infected with various viruses at day 0. (A) RCAS/AP (B) RCAS/Wnt5a (C) RCAS/Bmp4 (D) RCAS/Wnt-14.

(E) Peanut-agglutinin positive precartilage condensations in a day 3 MMC infected with RCAS/Wnt-14 at day 0.

(F) Lightly Alcian blue–stained cartilage nodules in a day 2 (untreated) MMC.

(G–J) Day 4 MMC treated with conditioned medium (CM) containing different viruses from day 2 onwards. (G) RCAS/AP-CM. (H) RCAS/Wnt5a-CM. (I) RCAS/Bmp4-CM. (J) RCAS/Wnt-14-CM.

AP cultures consistently showed a high-density distribution of strongly Alcian blue–stained cartilage nodules (Figure 3G). In contrast, cultures treated with medium containing *Wnt-14* virus showed significantly fewer cartilage nodules, which stained very lightly with Alcian blue (Figure 3J). Moreover, in most cases the number of Alcian blue–positive nodules at day 4 in *Wnt-14*-treated cultures was lower than in reference cultures fixed and stained at the time of infection (compare Figure 3F with 3J), suggesting that *Wnt-14* is able to cause reversion in Alcian blue staining in chondrogenic cells, as seen in normal joint initiation. Other factors, including *Wnt-5a* and *Bmp4*, did not have these in vitro effects (Figures 3B, 3C, 3H, and 3I)

#### Wnt-14 Induces Molecular Changes Characteristic of Joint Formation

To definitively determine whether *Wnt-14* induces subsequent changes characteristic of joint formation, we wanted to analyze molecular markers. Because the retroviral vector used is replication competent, it continues to spread. Thus, in our original infections done at day 3.5, the limbs became heavily infected and the skeletal elements were severely disrupted. For the molecular analysis, we injected the *Wnt-14* virus, at later stages, into individual digit rays. Since there was less time for viral spread, this allowed us to use the adjacent uninfected digits as internal controls. In individual digit rays infected this way, we observed phenotypic changes similar to those seen in the earlier infections, albeit in more localized regions (Figures 4A, 5A, 6A, and data not shown). The regions of densely packed, condensed mesenchyme present within the infected digits were indeed found to be expressing *Wnt-14*, using a probe that detects both exogenous and endogenous transcripts (Figures 4B, 5B, 5C, and 6B). When we aimed injections into the nonchondrogenic interdigital regions at stages 26–28, we did not observe similar phenotypic effects on the adjacent cartilage elements of the digits, nor did we observe morphological changes within the infected soft tissue (data not shown).

To address the molecular nature of the *Wnt-14*-infected, condensed mesenchymal regions, we first analyzed the expression of a number of genes that are known to be expressed in early prechondrogenic con-

densations, but which subsequently become downregulated in the developing joints. These included markers expressed in the early condensations, such as *Sox9* (Wright et al., 1995; Healy et al., 1996), *noggin* (Capdevila and Johnson, 1998), *collagen 2* (*Col2*; Koyama et al., 1995; Hurler and Colombatti, 1996; Nah et al., 1988), and the proteoglycan *aggrecan* (Wada et al., 1999), and others, such as the chondrocyte marker *collagen 9* (*Col9*; Swiderski and Solursh, 1992), which is not expressed in early chondrogenic condensations but which is specifically expressed in proliferating chondrocytes of the cartilage element. As shown in control sections, *Col9*, *Col2*, and *aggrecan* are completely absent from the normal joint-forming regions (Figures 4C, 6C, and 6G), while *Sox9* and *noggin* are expressed at significantly reduced levels in the joint interzone (see arrowheads in Figures 4E and 6E). Strikingly, a very similar pattern is seen in the *Wnt-14*-infected regions; the ectopic patches of condensed mesenchyme do not express *Col9*, *Col2*, or *aggrecan* (Figures 4D, 6D, and 6H), and express *Sox9* and *noggin* at substantially lower levels than the adjacent uninfected cartilage (Figures 4F and 6F). Both the absence of *Col9* and *Col2* expression and the low levels of *noggin* and *Sox9* in *Wnt-14*-infected areas are consistent with the hypothesis that the condensed mesenchyme represents chondrogenic cells that have become diverted to the joint phenotype.

To further analyze whether the condensed mesenchyme present in *Wnt-14*-infected regions truly reflects an interzone phenotype, we examined the expression of a number of genes that are normally expressed within developing joints. *Gli3* is one of several genes that are known to be expressed in the interzone of the joint, but which are also expressed in the perichondrium and in the mesenchyme surrounding the developing skeletal elements (Hui et al., 1994). Therefore, while *Gli3* was indeed upregulated in *Wnt-14*-infected regions (data not shown), this was not considered definitive evidence of a joint phenotype. However, we were able to exclude the possibility that these condensed mesenchymal cells were related to either perichondrial or mesenchymal cells by simultaneously analyzing *Bmp4* expression, which at these stages is expressed at high levels in the perichondrium and the interdigital mesenchyme, but is not yet expressed within the joint interzone (Figure 4G;

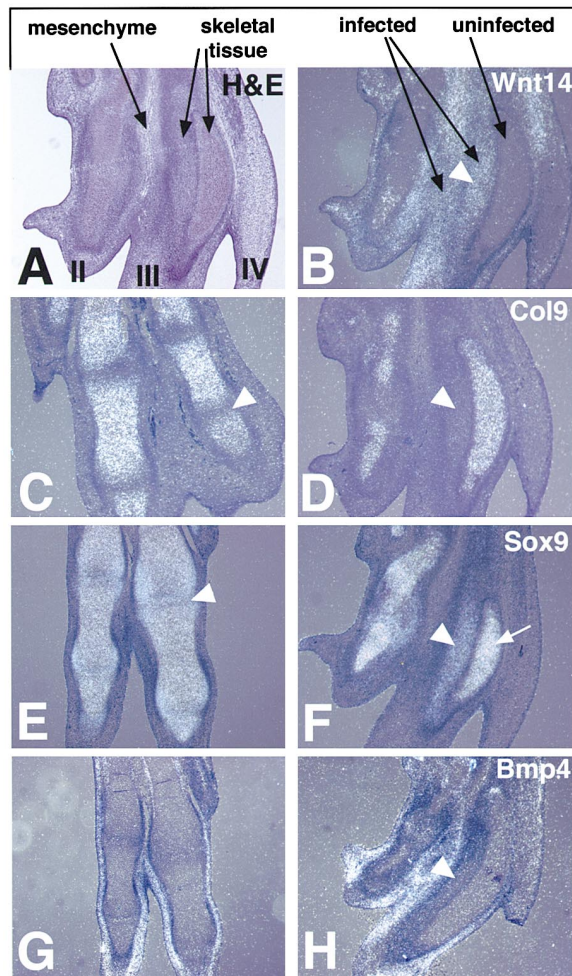


Figure 4. Infection of Chondrogenic Elements with *Wnt-14* Results in Downregulation of Chondrogenic Markers

H&E staining and radioactive in situ hybridizations on alternate sections through the foot region of an uninfected (C, E, and G) and an *Wnt-14*-infected (A, B, D, F, and H) leg at day 7.5 of development. (A) H&E staining of *Wnt-14*-infected autopod region showing aberrant morphology within the digit III region. Cells adjacent to the normal cartilage cells exhibit a distinctive condensed appearance. (B) In situ hybridization using a *Wnt-14* riboprobe detecting both endogenous and exogenous *Wnt-14*-transcripts. (C) Absence of *Col9* expression in the normal joint region (arrowhead). (D) No expression of *Col9* in the *Wnt-14*-infected condensed mesenchyme (arrowhead). (E) Low level of *Sox9* expression within the joint (arrowhead). (F) *Sox9* expression at low levels in the *Wnt-14*-infected condensed mesenchyme (arrowhead) and at high levels in the adjacent cartilage element (arrow). (G) *Bmp4* expression in the perichondrium and mesenchyme surrounding the digit elements. (H) *Bmp4* expression is not detected in the *Wnt-14*-infected condensed mesenchyme (arrowhead).

Francis-West et al., 1999b). Significantly, the *Wnt-14*-infected, condensed regions do not express *Bmp4* (arrowhead in Figure 4H), even though the adjacent mesenchyme does express the gene at high levels (Figure 4H).

Two markers that are specifically expressed in the joint interzone at these stages are the TGF $\beta$  superfamily

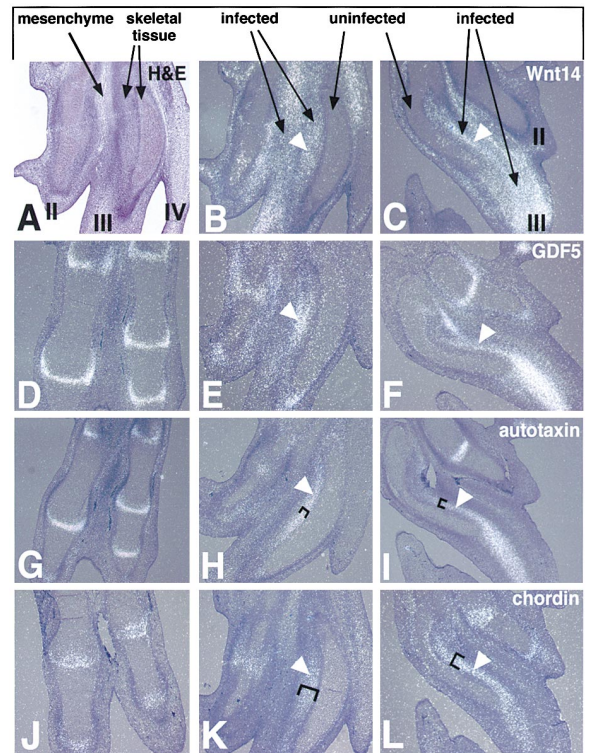


Figure 5. *Wnt-14* Misexpression Results in Induction of Joint-Specific Markers in Infected Chondrogenic Regions

H&E staining (A) and radioactive in situ hybridizations (B–L) on sections through the foot region of a chick limb at day 7.5 (stage 32–33) of development. (D, G, and J) Alternate sections through an uninfected contralateral control leg. (A, B, E, H, and K) Alternate sections of one *Wnt-14*-infected leg (note: alternate sections of the same legs are shown in Figures 4C–4H). (C, F, I, and L) Alternate sections of a second *Wnt-14*-infected limb. (A) H&E staining shows aberrant morphology of cells in the affected skeletal element (identical to section shown in Figure 4A). (B and C) Endogenous and exogenous *Wnt-14*-expression (arrowheads; note section shown in 5B is identical to 4B). (D) *Gdf5* expression in the normal joint. (E and F) Induced expression of *Gdf5* in the *Wnt-14*-infected skeletal tissue (arrowheads). (G) Expression of autotaxin in the joint interzone. (H and I) Induced expression of autotaxin in the *Wnt-14*-infected chondrogenic regions (arrowheads) in a narrow band (bracket). (J) Expression of *chordin* in all three layers of the joint interzone. (K and L) Induced expression of *chordin* in the *Wnt-14*-infected chondrogenic regions (arrowheads) in a broad domain (bracket).

member *Gdf5* (Figure 5D; Francis-West et al., 1999a; Merino et al., 1999) and the secreted phosphodiesterase/pyrophosphatase *autotaxin* (Figure 5G; Bächner et al., 1999). *Autotaxin* is not expressed in fibroblasts of the surrounding mesenchyme or in proliferating or differentiating chondrocytes of the cartilage elements in the chick limb. Significantly, both *Gdf5* (Figures 5E and 5F) and *autotaxin* (Figures 5H and 5I) are induced in *Wnt-14*-infected, condensed mesenchyme, consistent with the hypothesis that the infected region represents a joint interzone phenotype. However, since both genes, *autotaxin* and *Gdf5*, are also expressed in the early prechondrogenic mesenchyme (Chang et al., 1994; Francis-West et al., 1999a; R. Schweitzer, C. H., and C. J. T., unpublished observation), we cannot on the basis of this data alone exclude the possibility that *Wnt-14* mis-

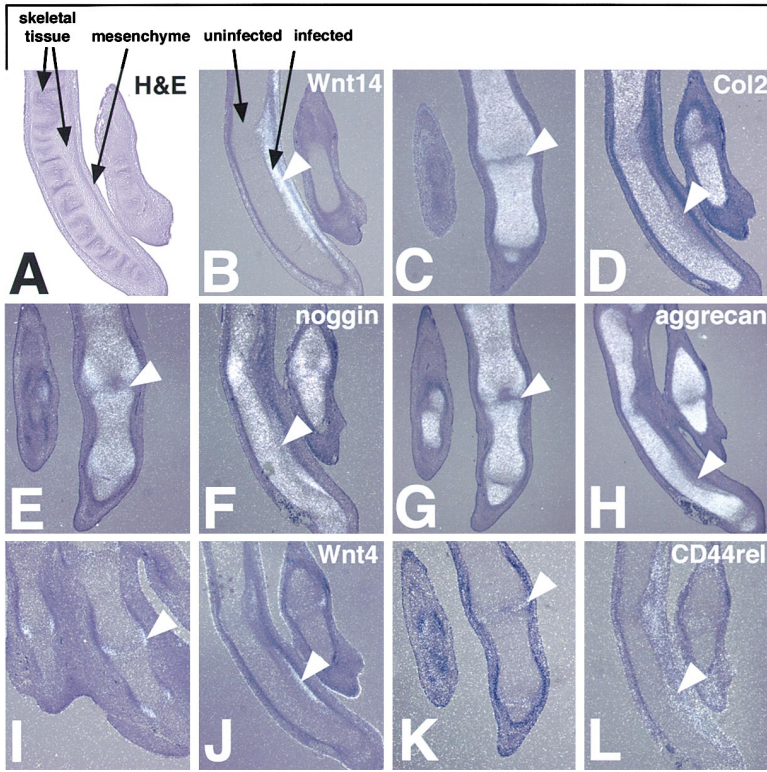


Figure 6. Analysis of Additional Chondrogenic and Joint Markers in a *Wnt-14*-Infected Digit III

H&E staining (A) and radioactive in situ hybridizations (B–L) on sections through the foot region of a chick limb at day 9 (stage 36) of development. (C, E, G, I, and K) Alternate sections through the digit III region in the uninfected contralateral leg. (A, B, D, F, H, J, and L) Alternate sections through a *Wnt-14*-infected digit III. (A) H&E staining showing aberrant morphology of *Wnt-14*-infected region. (B) Exogenous *Wnt-14* expression in the infected region within the skeletal element (arrowhead). (C) Absence of *Col2* expression from the normal joint interzone (arrowhead). (D) Absence of *Col2* expression in the *Wnt-14*-infected region (arrowhead). (E) Absence of *aggrecan* expression from the joint interzone (arrowhead). (F) Downregulated *aggrecan* expression in the *Wnt-14*-infected region (arrowhead). (G) Low-level expression of *noggin* in the joint interzone (arrowhead). (H) Low-level expression of *noggin* in the *Wnt-14*-infected region (arrowhead). (I) *Wnt-4* expression at the lateral edges of a wild-type joint (arrowhead). (J) Induced *Wnt-4* expression at the lateral edge of the *Wnt-14*-infected region (arrowhead). (K) Expression of *CD44rel* in the joint interzone (arrowhead). (L) Upregulation of *CD44rel* expression throughout the *Wnt-14*-infected region (arrowhead).

expression simply arrests cells in a prechondrogenic state. We therefore expanded our analysis by examining the expression of several additional genes that are not expressed in the prechondrogenic mesenchyme but are specifically associated with forming joints, including *chordin*, which is expressed specifically in the interzone (Figure 5J; Francis-West et al., 1999b), *Wnt-4*, which is normally expressed at the lateral edges of the developing joints (Figure 6I; Hartmann and Tabin, 2000), and *CD44rel*, a gene related to human CD44 which, like CD44 (Edwards et al., 1994), is expressed by joint interzone cells (Figure 6K). Strikingly, we find that each of these additional joint specific markers—*chordin* (Figures 5L and 5M), *Wnt-4* (Figure 6J), and *CD44rel* (Figure 6L)—is specifically induced in *Wnt-14*-infected chondrogenic regions.

Finally, it is also worth noting that several of the interzone markers described above have distinct distribution patterns within the joint. For example, *chordin* is expressed in all three layers of the interzone, with slightly higher expression levels in the two outer layers (Figure 5J). By contrast, *autotaxin* expression is confined to the middle layer of the interzone (Figure 5G), while *Wnt-4* expression is restricted to the lateral edges (Figure 6I). The *Wnt-14*-infected regions recapitulate this pattern, with *autotaxin* confined to a relatively narrow strip of cells nested within a much broader domain of *chordin* expression (compare Figure 5H with 5K), and *Wnt-4* expressed only at the edge facing the adjacent mesenchyme (Figure 6J). Thus, the spatial expression of these genes, together with the histological and molecular data presented above, strongly argues that the *Wnt-14*-infected region is induced to take on an interzone-like phenotype.

### Endogenous Joint Formation Is Repressed in Regions Adjacent to Ectopic *Wnt-14* Expression

An important aspect of skeletal patterning is the spacing of the joints. Joints in the limb form sequentially, in a proximal to distal sequence (Shubin and Alberch, 1986). As a possible mechanism for achieving the spacing between joints, one could postulate that signals could be produced by a newly formed joint interzone that blocks the initiation of a new segmentation event in the adjacent precartilagenous element, with the more distal joints only forming at locations distal enough to escape the influence of the previously formed joint. Consistent with this, we found that in every example of infection with the replication-competent virus, ectopic *Wnt-14* expression prevented expression of all of the examined joint markers in adjacent uninfected cartilage regions where the endogenous joints normally should have formed (Figures 7A and 7B). Importantly, the chondrogenic regions were otherwise normal in histology and showed no evidence of overproliferation (Figure 7B).

There are reports that the BMP antagonist Noggin is capable of altering the process of joint formation, for example converting a digit 3, which normally has three phalanges, to a digit 2-like element containing only two phalanges (Dahn and Fallon, 2000). One would expect that if there is a change in location or number of joints, it would be reflected by an earlier alteration in the expression of joint markers, including *Wnt-14*. We implanted Noggin beads into the distal region of the interdigital region between digits 3 and 4 in the leg at stage 27–28 and replicated the previously published result, and moreover observed the predicted changes in *Wnt-14* expression (data not shown). However, the signifi-

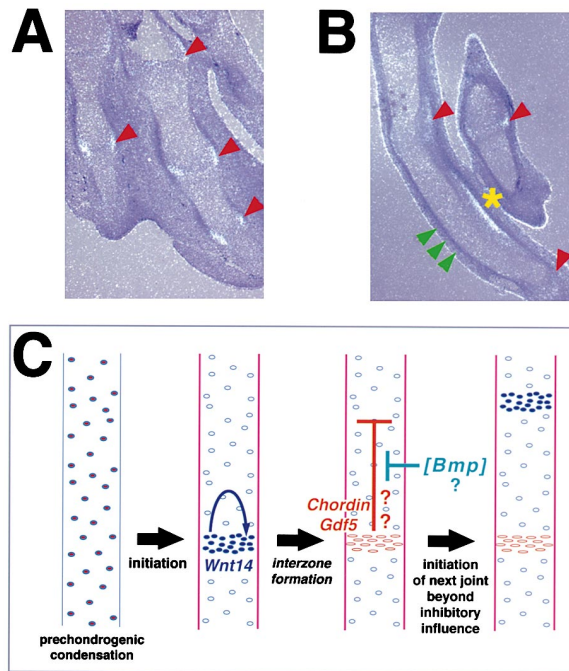


Figure 7. *Wnt-14* Misexpression Represses Adjacent Joints

(A) Normal spacing of joints visualized by the expression of *Wnt-4* in the lateral edges of the joints in an uninfected control leg (red arrowheads).

(B) Repression of endogenous joint formation (green arrowheads) in the region adjacent to *Wnt-14*-infection. *Wnt-14* induces lateral expression of *Wnt-4* (yellow asterisk). The more proximal and distal joints (red arrowheads) are formed, but also slightly affected.

(C) Model of spacing of the joints. The initial step of joint formation involves induction of *Wnt-14* expression, this leads to the formation of the interzone characterized by distinct gene expression patterns, including expression of *Gdf5* and *Chordin*. Secondary signals secreted from the interzone, which could include either *Gdf5* or *Chordin* (see text) act on neighboring cartilage elements to prevent the induction of a new interzone in the vicinity. These signals may be under a modulating influence of signals (such as BMPs) emanating from the interdigital mesenchyme (see text).

cance of this observation is unclear (see discussion below).

## Discussion

In this study, we report the analysis of *Wnt-14*, a member of the *Wnt* gene family, which shows a striking pattern of expression within the early joint-forming regions of the developing chick limb. By misexpressing *Wnt-14* locally within the developing autopod, we show that cells within prechondrogenic regions respond to exogenous *Wnt-14* by becoming morphologically and histologically distinct from neighboring cartilage and adjacent mesenchymal cells, taking on histological and molecular properties typical of the early joint interzone. All genes examined that are expressed in the normal joint interzone but not in the adjacent cartilage were expressed in *Wnt-14*-infected skeletal tissue; conversely, all genes downregulated in the normal interzone were repressed by *Wnt-14*. Note that the set of markers expressed following *Wnt-14* misexpression is characteristic of the

early interzone, not of the mature joint or articular cartilage, although some individual markers continue to be expressed in the mature joint, such as *Gdf5* and *Col2*. Based on all these consistent changes in the histological and molecular phenotype induced by *Wnt-14*, we propose a role for *Wnt-14* in the initial steps of joint formation (Figure 7C).

Consistent with the *in vivo* data, *Wnt-14* can block cartilage differentiation in micromass cultures *in vitro* when added at the beginning of the culture period and can cause a reversal of cartilage differentiation when added later. The former property of blocking chondrogenesis in micromass cultures have also been reported for *Wnt-1* and *Wnt-7a* (Rudnicki and Brown, 1997; Stott et al., 1999); however, these Wnts are not normally expressed in developing joints and their misexpression does not produce any of the subsequent changes characteristic of joint formation (Rudnicki and Brown, 1997; C. H. and C. J. T., unpublished observation). This ability of *Wnt-14* to block or even reverse chondrogenesis may be an essential property for allowing cells to enter the alternative interzone differentiation pathway.

*Wnt-14* is able to actively direct prechondrogenic cells into the joint-forming pathway. This effect is clearly seen *in vivo* in the ability of *Wnt-14* to induce the expression of a number of molecular markers characteristic of the developing joint. The induction of *CD44rel* in the ectopic joint region is interesting, since CD44, which is the major hyaluronan (HA)-binding protein, has been implicated in playing a role in the subsequent development of the joint (reviewed by Pitsillides, 1999).

Notably, however, ectopic *Wnt-14* is not capable of inducing any of the joint markers in nonchondrogenic cell types such as the interdigital mesenchyme, indicating that only chondrogenic cells are competent to respond to the joint-inducing properties of *Wnt-14*. In this regard, we note that endogenously, *Wnt-14* is, in fact, expressed in mesenchymal cells outside of the perichondrium flanking the cartilage elements. It is possible that although these cells cannot be stimulated to become interzone cells, they may be capable of responding to the first of the two *Wnt-14* activities described above, blocking them from entering the chondrogenic pathway and hence limiting the thickness of the cartilagenous condensations. In any case, *Wnt* proteins typically remain in very close proximity to the cells that produce them, and hence this interdigital *Wnt-14* would not be expected to transverse the perichondrium and to act on the chondrocytes.

## Wnt-14 Signal Transduction

A variety of different signaling pathways involved in the intracellular transduction of *Wnt* signals have been identified in recent years (for reviews, see Cox and Peifer, 1998; Arias et al., 1999; Dierick and Bejsovec, 1999; Miller et al., 1999; Mlodzik, 1999; Kühl et al., 2000). *Wnt-14* is likely to use a signaling pathway distinct from other *Wnt* genes known to play roles in skeletogenesis, such as *Wnt-4* and *Wnt-5a*, because their misexpression leads to completely different phenotypes (Hartmann and Tabin, 2000). We attempted to determine which of the previously described *Wnt* signaling pathways might be responsible for transducing the *Wnt-14* signal in joint

formation, misexpressing activated versions of  $\beta$ -catenin, RhoA, and CamKII and a dominant-negative version of Dishevelled, but none of these gave rise to a phenotype indicative of the pathway utilized by Wnt-14 (data not shown).

### Spacing of the Joints

We have found that ectopic *Wnt-14* expression also leads to a repression of joint formation in adjacent cartilage. This provides a potential mechanism for spacing the joints, where each newly formed joint would block formation of additional joints in its immediate vicinity (Figure 7C). There are two previously reported results, either or both of which could potentially indicate a downstream cascade in this process.

Gdf5 is a secreted member of the BMP superfamily which we find to be induced by Wnt-14 in the ectopic interzone-like region. Previous studies have shown that Gdf5 bead implants or misexpression of this joint marker result in a fusion of the skeletal elements (Francis-West et al., 1999a; Merino et al., 1999; Storm and Kingsley, 1999). Gdf5 thus could be a secondary signal produced downstream of Wnt-14 that blocks secondary joint formation (Figure 7C). It should be noted, however, that Gdf5 has a strong proliferative effect on the cartilage and the elements forming adjacent to a source of Gdf5 are significantly enlarged, in contrast to the normal appearance of cartilage adjacent to the ectopic *Wnt-14* expression. Thus, the apparent block in the joint formation following Gdf5 application could be a consequence of cartilage overgrowth, or redirection of joint cells down the chondrogenic pathway not necessarily indicative of an endogenous joint-repressing activity.

Another potential pathway influencing joint positioning involves interdigital BMP activities. The interdigital region has been shown to influence the number of phalanges that form and application of ectopic noggin reduces the number of skeletal elements in the adjacent digit (Dahn and Fallon, 2000). We have repeated this result and indeed see a concomitant change in *Wnt-14* expression in the altered digit. The decrease in the number of phalanges following exogenous application of the BMP antagonist Noggin implies that endogenous interdigital BMPs might act to promote joint formation. In this case, a BMP antagonist produced by the forming joint could serve to block the formation of new joints in close proximity of the newly formed joint. Consistent with this model, we find that the BMP-antagonist *chordin* is specifically upregulated in the early joint interzone in response to *Wnt-14*, and hence could be a secondary signal responsible for the spacing of the joints (Figure 7C). However, the cellular mechanism responsible for the effect of ectopic Noggin on joint spacing has not been reported. In this regard it must be noted that application of Noggin beads do not result in larger skeletal elements that are simply missing joints, but rather in the apparent loss of phalanges such that fewer segments are present. From our own observations in replicating these experiments, we strongly favor the hypothesis that ectopic Noggin produces the described phenotypes by interfering with the chondrogenesis-promoting activity of BMP signaling such that the condensation of the distal phalanx is either delayed or pre-

vented and fewer segments are produced, not that it has a direct effect on the spacing of joint formation. Further work will be required to clarify the roles of *Gdf5* and *chordin* downstream of Wnt-14 and to determine whether either of them plays a role in the endogenous spacing of the joints.

### Later Functions of Wnt-14 in the Mature Joint

*Wnt-14* continues to be expressed in structures associated with the mature joint, in areas of the capsule and throughout the synovial membrane. This expression will be particularly intriguing to consider in the context of rheumatoid arthritis (RA), which is associated with alterations of the synovium and is one of the most common diseases of the joint. There is growing evidence that Wnt signaling may be involved in some specific pathological alterations of the joint. Recent studies have shown that transcripts of certain Wnt genes, along with certain members of the *Frizzled* family of Wnt receptors, can be found within the RA synovium, and that some of these genes are specifically upregulated in the RA synovia (Sen et al., 2000). Hurvitz and colleagues (1999) have further shown that mutations in *WISP3*, a member of the CCN family of secreted, cysteine-rich growth factors, cause progressive pseudorheumatoid dysplasia (PPD), a disease that resembles RA phenotypically. The highly related *WISP* genes, *WISP1* and *WISP2*, were originally identified as Wnt-1-responsive genes (Pennica et al., 1998; Xu et al., 2000). These findings do suggest a possible role for Wnt signaling in the etiology of RA. Since Wnt-14 is involved in the induction of the synovial joints and continues to be expressed in the mature joint, Wnt-14 might play a positive role in the maintenance of joint integrity. Determining whether Wnt-14 signaling is involved in any synovial joint disease will be an important target of future studies.

### The Process of Joint Formation

The formation of the joint constitutes a complex, multistep process. It begins with the arrest of chondrogenic differentiation in the prospective joint interzone, marked by the disappearance of collagen type II (Koyama et al., 1995; Hurler and Colombatti, 1996). The next steps involve further changes in the matrix (Pitsillides et al., 1995), accompanied by cell death (Mori et al., 1995), and ultimately the formation of the mature joint cavity. Concomitantly, the articular cartilage and joint capsule differentiate around the joint cavity (Mitrovic, 1977). Wnt-14 plays a role at the earliest step in this process, the induction of the joint interzone. Significantly, at least some secondary signals appear to be initiated as a consequence of *Wnt-14* expression. For example, *Gdf5* is a secreted signal necessary for joint formation produced in response to Wnt-14. Moreover, we have observed that distinct zones of the joint interzone express characteristic molecular markers, and that these distinct regions of differential gene expression are recapitulated following *Wnt-14* misexpression. Nevertheless, it is still unclear whether Wnt-14 is sufficient to trigger all of the subsequent steps in producing a mature joint. Given the fact that joint development is a complex process, it is more than likely that additional signals are necessary in order to produce a mature joint.

Our analysis of later stages of joint development is complicated by the fact that the replication-competent retrovirus continues to spread further with progression of the experiment, producing an ever-larger interzone domain. The joint interzone normally develops between two closely juxtaposed cartilage elements, an architecture which is therefore missing in our *Wnt-14* misexpression experiments. Significantly, cross-talk between the cartilage and the interzone is known to be important for later steps of joint development, including cavitation (Holder, 1977). The discovery that *Wnt-14* can induce the initial steps in joint formation thus sets the stage for identifying additional secondary signals required for the subsequent stages of joint maturation. Such studies, elaborating on the current work, will have important implications, both potentially from a clinical perspective, as joint disease is a major human health problem, as well as from the developmental biology perspective, as the locations where joints arise is a major determinant of the final skeletal pattern.

#### Experimental Procedures

##### RNA Probes

Antisense riboprobes radiolabeled with [<sup>32</sup>P]UTP were prepared as described as follows: *Col9*, *Bmp4*, *noggin*, and *chordin* (Pathi et al., 1999), *Gli3* (Schweitzer et al., 2000), *Sox9* (Healy et al., 1996), and *Wnt-4* (Hartmann and Tabin, 2000). DNA fragments corresponding to *Wnt-14* (Bergstein et al., 1997; full-length open reading frame), *Col2* (Nah et al., 1988; 434 bp fragment corresponding to nucleotides 182–616 of GenBank sequence #M74435), *aggrecan* (687 bp fragment corresponding to nucleotides 113–800 of GenBank sequence #L21913) and *CD44rel* (470 bp fragment corresponding to nucleotides 814–1284 of GenBank sequence #AF153205) were amplified by RT-PCR and cloned into pGEM-T. A chick *Gdf5* template, corresponding to amino acids 285–411 of mouse GDF5, was amplified by RT-PCR using degenerate primers and cloned into pGEM-T. Riboprobes for *Wnt-14*, *CD44rel*, *Gdf5*, and *autotaxin* were generated using T7 RNA polymerase from templates linearized with *SpeI* or, in the case of *autotaxin*, with *NcoI*. Riboprobes for *Col2* and *aggrecan* were generated using *Sp6* RNA polymerase from templates linearized with *NcoI*.

##### Processing of Chick Embryos and In Situ Hybridization

Embryos were staged according to Hamburger and Hamilton (1951), fixed in 4% paraformaldehyde/PBS (pH 7.4) for 6–8 hours, or overnight at 4°C, and processed for either whole embryo skeletal staining or paraffin sectioning. For radioactive section in situ hybridizations on serial sections, two continuous 5 μm microtome sections of paraffin-embedded uninjected contralateral (left) and virally-infected (right) limbs (treated in parallel and embedded into the same mold) were successively collected onto 5–8 alternating slides and processed as described (Hartmann and Tabin, 2000).

##### Construction of Retroviral Constructs and Viral Misexpression

The RCASBP(A) constructs carrying the full-length open reading frame of the chick *Wnt-14* gene (5' *NcoI*: TGCCATGGCTCTCTCC GCGCGCTTCTTAGG; 3' *EcoRI*: CGGAATTCAGTCTTTACAGGTG TAAACC), the activated form of *Drosophila* RhoA-V14 (5' *BsaI*: GGTCTCCATGACGACGATTGCG; 3' *EcoRI*: CGGAATTCAGAGCA AAAGGCATC), the activated form of *CamKII* (5' *NcoI*: TGTCACC ATGGCTACCATCACCTGC; 3' *EcoRI*: GTGAATTC AATGGGGCAG GACGG) and the dominant-negative form of *Dishevelled* (5' *BsmBI*: CGTCTCACATGGAGAGCTTGGGCGACC; 3' *HindIII*: TGTAAGCTT CACATGACATCCACAAGAAG) were engineered as outlined in Logan and Tabin (1998). Transfection and growth of RCAS viruses were performed as described by Morgan and Fekete (1996). Concentrated virus with a titer of 6–8 × 10<sup>8</sup> pfu/ml was injected either into the posterior regions of the developing wing at day 3.5 (stage 21–22)

or into the distal region of digit III of the foot at day 5 (stage 26–27). In both instances, the uninjected, contralateral limbs served as stage-specific controls.

##### Bead Implants

Affigel Blue agarose beads (Biorad) were washed in PBS and soaked in Noggin protein on ice (concentrations were 200, 500, or 700 μg/ml). Similar results were obtained independent of the concentration used. Noggin loaded beads were implanted in the distal most avascular region of the interdigital mesenchyme between digit 3 and 4 of the leg at stage 27–28 according to Dahn and Fallon (2000).

##### Skeletal Staining, Histology, and Immunohistochemistry

Whole-mount Alcian blue staining of cartilage elements of day 9.5 chick embryos was done as previously described in Goff and Tabin (1997). Weigert-SafraninO staining of sections was done according to Gaffney (1994) and H&E staining according to Allen (1994). For immunohistochemical analysis, sections were deparaffinized (10 min Xylene), and rehydrated (100%, 85%, 70%, 50%, and 25% EtOH) into PBS, and endogenous peroxidase activity was inactivated through incubation in 3% H<sub>2</sub>O<sub>2</sub> in methanol for 30 min. Sections were then incubated with a 1:2 diluted 3b2 monoclonal antibody specific for type III collagen (R. Mayne; obtained from the Developmental Studies Hybridoma Bank) and developed using a biotinylated horse-anti-mouse secondary antibody (Vector), horseradish peroxidase-conjugated streptavidin complexes (Vector), and Diaminobenzidine for the color reaction (Sigma). Sections were also counterstained with hematoxylin (Sigma).

##### Micromass Cultures

Micromass cultures were carried out as described by Zou et al. (1997) using stage 22–23 fore- and hindlimb buds with the following modifications: Ectoderm was removed after a 15 min incubation in 0.2 M EDTA/PBS at 37°C, and mesenchymal cells were then dissociated and plated at a density of 2 × 10<sup>7</sup> cells/ml. For infections on day 0, 10 μl aliquots of cell suspensions were infected with 1 μl of concentrated RCAS virus encoding either human *alkaline phosphatase* (for control cultures), *Wnt-5a*, *Bmp4*, or *Wnt-14*. For each virus, two cultures were plated together on four-well 10 mm tissue culture dishes (Nunc), and following one hour of incubation, 500 μl of DMEM containing 10% fetal calf serum and 2% chick serum was added. For infections on day 2, 10 μl aliquots of the mesenchymal cell suspension were plated onto four-well 10 mm tissue culture dishes and then incubated for 2 days, at which point a set of reference cultures were fixed (4% paraformaldehyde/PBS), while medium supplemented 1:1 with sterile-filtered conditioned media from DF1 cells infected either with RCAS-AP, RCAS-*mWnt-5a*, RCAS-*Bmp4*, or RCAS-*Wnt-14* was added to control and experimental cultures, respectively. Cells were further cultured for two more days, with fresh conditioned medium added twice daily and then fixed on day 4. In all cases, cultures were stained with Alcian blue (pH 1) to visualize chondrogenic nodule formation. Peanut-agglutinin staining was done as previously described by Rudnicki and Brown (1997) using biotinylated peanut-agglutinin (Vector). For each experiment, at least four cultures of each type were analyzed, and each experiment was repeated three times with similar results.

##### Acknowledgments

We thank G. Kardon, R. Schweitzer, and specifically K. Vogan for critical reading of this manuscript. We further thank Vicki Rosen for the recombinant Noggin protein. C. H. was supported by a postdoctoral fellowship from the Human Frontiers Science Program. This work was supported by a program project grant from the NIH.

Received September 7, 2000; revised January 5, 2001.

##### References

- Ahrens, P.B., Solursh, M., and Reiter, R.S. (1977). Stage related capacity for limb chondrogenesis in cell culture. *Dev. Biol.* 60, 69–82.
- Allen, T.C. (1994). Hematoxylin and eosin. In *Laboratory Methods in Histotechnology* (Armed Forces Institute of Pathology), Prophet,

- E.B., Mills, B., Arrington, J.B., and Sobin, L.H., eds. (Washington, D.C., American Registry of Pathology), pp. 53–57.
- Arias, A.M., Brown, A.M., and Brennan, K. (1999). Wnt signalling: pathway or network? *Curr. Opin. Genet. Dev.* 9, 447–454.
- Bächner, D., Ahrens, M., Betat, N., Schroder, D., and Gross, G. (1999). Developmental expression analysis of murine autotaxin (ATX). *Mech. Dev.* 84, 121–125.
- Ballard, K.J., and Holt, S.J. (1968). Cytological and cytochemical studies on cell death and digestion in the foetal rat foot: the role of macrophages and hydrolytic enzymes. *J. Cell Sci.* 3, 245–262.
- Bergstein, I., Eisenberg, L.M., Bhalerao, J., Jenkins, N.A., Copeland, N.G., Osborne, M.P., Bowcock, A.M., and Brown, A.M. (1997). Isolation of two novel WNT genes, WNT-14 and WNT15, one of which (WNT15) is closely linked to WNT3 on human chromosome 17q21. *Genomics* 46, 450–458.
- Capdevila, J., and Johnson, R.L. (1998). Endogenous and ectopic expression of noggin suggests a conserved mechanism for regulation of BMP function during limb and somite patterning. *Dev. Biol.* 197, 205–217.
- Chang, S.C., Hoang, B., Thomas, J.T., Vukicevic, S., Luyten, F.P., Ryba, N.J., Kozak, C.A., Reddi, A.H., and Moos, M., Jr. (1994). Cartilage-derived morphogenetic proteins. New members of the transforming growth factor-beta superfamily predominantly expressed in long bones during human embryonic development. *J Biol Chem* 269, 28227–28234.
- Cox, R.T., and Peifer, M. (1998). Wingless signaling: the inconvenient complexities of life. *Curr. Biol.* 8, 140–144.
- Craig, F.M., Bentley, G., and Archer, C.W. (1987). The spatial and temporal pattern of collagens I and II and keratan sulphate in the developing chick metatarsophalangeal joint. *Development* 99, 383–391.
- Dahn, R.D., and Fallon, J.F. (2000). Interdigital regulation of digit identity and homeotic transformation by modulated BMP signaling. *Science* 289, 438–441.
- Dierick, H., and Bejsovec, A. (1999). Cellular mechanisms of wingless/Wnt signal transduction. *Curr. Topics Dev. Biol.* 43, 153–190.
- Edwards, J.C., Wilkinson, L.S., Jones, H.M., Soothill, P., Henderson, K.J., Worrall, J.G., and Pittsillides, A.A. (1994). The formation of human synovial joint cavities: a possible role for hyaluronan and CD44 in altered interzone cohesion. *J. Anat.* 185, 355–367.
- Francis-West, P.H., Abdelfattah, A., Chen, P., Allen, C., Parish, J., Lather, R., Allen, S., MacPherson, S., Luyten, F.P., and Archer, C.W. (1999a). Mechanisms of GDF-5 action during skeletal development. *Development* 126, 1305–1315.
- Francis-West, P.H., Parish, J., Lee, K., and Archer, C.W. (1999b). BMP/GDF-signalling interactions during synovial joint development. *Cell Tissue Res.* 296, 111–119.
- Gaffney, E. (1994). Carbohydrates. In *Laboratory Methods in Histochemistry* (Armed Forces Institute of Pathology), Prophet, E.B., Mills, B., Arrington, J.B., and Sobin, L.H., eds. (Washington, D.C., American Registry of Pathology), pp. 149–174.
- Goff, D.J., and Tabin, C.J. (1997). Analysis of Hoxd 13 and Hoxd 11 misexpression in chick limb buds reveals that Hox genes affect both bone condensation and growth. *Development* 124, 627–636.
- Grüneberg, H., and Lee, A.J. (1973). The anatomy and development of brachypodism in the mouse. *J. Embryol. Exp. Morphol.* 30, 119–141.
- Hall, B.K., and Miyake, T. (1995). Divide, accumulate, differentiate: cell condensation in skeletal development revisited. *Int. J. Dev. Biol.* 39, 881–893.
- Hall, B.K., and Miyake, T. (2000). All for one and one for all: condensations and the initiation of skeletal development. *Bioessays* 22, 138–147.
- Hamburger, V., and Hamilton, H.L. (1951). A series of normal stages in the development of the chick embryo. *J. Morphol.* 88, 49–92.
- Hartmann, C., and Tabin, C.J. (2000). Dual roles of wnt signaling during chondrogenesis in the chicken limb. *Development* 127, 3141–3159.
- Healy, C., Uwanogho, D., and Sharpe, P.T. (1996). Expression of the chicken Sox9 gene marks the onset of cartilage differentiation. *Ann. NY Acad. Sci.* 785, 261–262.
- Hinchliffe, J.R. (1994). Evolutionary developmental biology of the tetrapod limb. *Development (Suppl)*, 163–168.
- Hinchliffe, J.R., and Johnson, D.R. (1980). *The Development of the Vertebrate Limb* (Oxford: Clarendon Press).
- Holder, N. (1977). An experimental investigation into the early development of the chick elbow joint. *J. Embryol. Exp. Morphol.* 39, 115–127.
- Hui, C.C., Slusarski, D., Platt, K.A., Holmgren, R., and Joyner, A.L. (1994). Expression of three mouse homologs of the Drosophila segment polarity gene cubitus interruptus, Gli, Gli 2, and Gli 3, in ectoderm and mesoderm derived tissues suggests multiple roles during postimplantation development. *Dev. Biol.* 162, 402–413.
- Hurle, J.M., and Colombatti, A. (1996). Extracellular matrix modifications in the interdigital spaces of the chick embryo leg bud during the formation of ectopic digits. *Anat. Embryol.* 193, 355–364.
- Hurvitz, J.R., Suwairi, W.M., Van Hul, W., El-Shanti, H., Superti-Furga, A., Roudier, J., Holderbaum, D., Pauli, R.M., Herd, J.K., Van Hul, E.V., et al. (1999). Mutations in the CCN gene family member WISP3 cause progressive pseudorheumatoid dysplasia. *Nat. Genet.* 23, 94–98.
- Izpisua-Belmonte, J.C., and Duboule, D. (1992). Homeobox genes and pattern formation in the vertebrate limb. *Dev. Biol.* 152, 26–36.
- Johnson, R.L., Riddle, R.D., and Tabin, C.J. (1994). Mechanisms of limb patterning. *Curr. Opin. Genet. Dev.* 4, 535–542.
- Kawakami, Y., Wada, N., Nishimatsu, S.I., Ishikawa, T., Noji, S., and Nohno, T. (1999). Involvement of Wnt 5a in chondrogenic pattern formation in the chick limb bud. *Dev. Growth Differ.* 41, 29–40.
- Kimura, S., and Shiota, K. (1996). Sequential changes of programmed cell death in developing fetal mouse limbs and its possible roles in limb morphogenesis. *J. Morphol.* 229, 337–346.
- Koyama, E., Leatherman, J.L., Shimazu, A., Nah, H.D., and Pacifici, M. (1995). Syndecan 3, tenascin C, and the development of cartilaginous skeletal elements and joints in chick limbs. *Dev. Dyn.* 203, 152–162.
- Kühl, M., Sheldahl, L.C., Park, M., Miller, J.R., and Moon, R.T. (2000). The Wnt/Ca<sup>2+</sup> pathway: a new vertebrate Wnt signaling pathway takes shape. *Trends Genet.* 16, 279–283.
- Landauer, W. (1952). Brachypodism: A recessive mutation of house-mice. *J. Hered.* 43, 724–732.
- Logan, M., and Tabin, C. (1998). Targeted gene misexpression in chick limb buds using avian replication competent retroviruses. *Methods* 14, 407–420.
- Merino, R., Macias, D., Ganan, Y., Economides, A.N., Wang, X., Wu, Q., Stahl, N., Sampath, K.T., Varona, P., and Hurle, J.M. (1999). Expression and function of Gdf 5 during digit skeletogenesis in the embryonic chick leg bud. *Dev. Biol.* 206, 33–45.
- Miller, J.R., Hocking, A.M., Brown, J.D., and Moon, R.T. (1999). Mechanism and function of signal transduction by the Wnt/beta catenin and Wnt/Ca<sup>2+</sup> pathways. *Oncogene* 18, 7860–7872.
- Mitrovic, D.R. (1977). Development of the metatarsophalangeal joint of the chick embryo: morphological, ultrastructural and histochemical studies. *Am. J. Anat.* 150, 333–347.
- Mlodzik, M. (1999). Planar polarity in the Drosophila eye: a multifaceted view of signaling specificity and cross-talk. *EMBO J.* 18, 6873–6879.
- Morgan, B.A., and Fekete, D.M. (1996). Manipulating gene expression with replication-competent retroviruses. *Methods Cell. Biol.* 51, 185–218.
- Mori, C., Nakamura, N., Kimura, S., Irie, H., Takigawa, T., and Shiota, K. (1995). Programmed cell death in the interdigital tissue of the fetal mouse limb is apoptosis with DNA fragmentation. *Anat. Rec.* 242, 103–110.
- Nah, H.D., Rodgers, B.J., Kulyk, W.M., Kream, B.E., Kosher, R.A., and Upholt, W.B. (1988). In situ hybridization analysis of the expression of the type II collagen gene in the developing chicken limb bud. *Coll. Relat. Res.* 8, 277–294.

- Nalin, A.M., Greenlee, T.K., Jr., and Sandell, L.J. (1995). Collagen gene expression during development of avian synovial joints: transient expression of types II and XI collagen genes in the joint capsule. *Dev. Dyn.* 203, 352–362.
- Oster, G.F., Shubin, N., Murray, J.D., and Alberch, P. (1988). Evolution and morphogenetic rules: The shape of the vertebrate limb in ontogeny and phylogeny. *Evolution* 42, 862–884.
- Pathi, S., Rutenberg, J.B., Johnson, R.L., and Vortkamp, A. (1999). Interaction of Ihh and BMP/Noggin signaling during cartilage differentiation. *Dev. Biol.* 209, 239–253.
- Pennica, D., Swanson, T.A., Welsh, J.W., Roy, M.A., Lawrence, D.A., Lee, J., Brush, J., Taneyhill, L.A., Deuel, B., Lew, M., et al. (1998). WISP genes are members of the connective tissue growth factor family that are up regulated in wnt 1 transformed cells and aberrantly expressed in human colon tumors. *Proc. Natl. Acad. Sci. USA* 95, 14717–14722.
- Pitsillides, A.A. (1999). The role of hyaluronan in joint cavitation. In *The Biology of the Synovial Joint*, C.W. Archer, B. Caterson, J. Ralphs, and M. Benjamin, eds. (London, Harwood Academics), pp. 41–61.
- Pitsillides, A.A., Archer, C.W., Prehm, P., Bayliss, M.T., and Edwards, J.C. (1995). Alterations in hyaluronan synthesis during developing joint cavitation. *J. Histochem. Cytochem.* 43, 263–273.
- Polinkovsky, A., Robin, N.H., Thomas, J.T., Irons, M., Lynn, A., Goodman, F.R., Reardon, W., Kant, S.G., Brunner, H.G., van der Burgt, I., et al. (1997). Mutations in CDMP1 cause autosomal dominant brachydactyly type C. *Nat. Genet.* 17, 18–19.
- Ros, M.A., Rivero, F.B., Hinchliffe, J.R., and Hurle, J.M. (1995). Immunohistological and ultrastructural study of the developing tendons of the avian foot. *Anat. Embryol.* 192, 483–496.
- Rudnicki, J.A., and Brown, A.M. (1997). Inhibition of chondrogenesis by Wnt gene expression in vivo and in vitro. *Dev. Biol.* 185, 104–118.
- Schweitzer, R., Vogan, K.J., and Tabin, C.J. (2000). Similar expression and regulation of Gli2 and Gli3 in the chick limb bud. *Mech. Dev.* 98, 171–174.
- Sen, M., Lauterbach, K., El-Gabalawy, H., Firestein, G.S., Corr, M., and Carson, D.A. (2000). Expression and function of wingless and frizzled homologs in rheumatoid arthritis. *Proc. Natl. Acad. Sci. USA* 97, 2791–2796.
- Shubin, N.H., and Alberch, P. (1986). A morphogenetic approach to the origin and basic organization of the tetrapod limb. *Evolutionary Biol.* 20, 319–387.
- Storm, E.E., and Kingsley, D.M. (1996). Joint patterning defects caused by single and double mutations in members of the bone morphogenetic protein (BMP) family. *Development* 122, 3969–3979.
- Storm, E.E., and Kingsley, D.M. (1999). GDF5 coordinates bone and joint formation during digit development. *Dev. Biol.* 209, 11–27.
- Storm, E.E., Huynh, T.V., Copeland, N.G., Jenkins, N.A., Kingsley, D.M., and Lee, S.J. (1994). Limb alterations in brachypodism mice due to mutations in a new member of the TGF beta superfamily. *Nature* 368, 639–643.
- Stott, N.S., Jiang, T.X., and Chuong, C.M. (1999). Successive formative stages of precartilaginous mesenchymal condensations in vitro: modulation of cell adhesion by Wnt 7A and BMP 2. *J. Cell Physiol.* 180, 314–324.
- Swiderski, R.E., and Solorsh, M. (1992). Differential co expression of long and short form type IX collagen transcripts during avian limb chondrogenesis in ovo. *Development* 115, 169–179.
- Thomas, J.T., Lin, K., Nandedkar, M., Camargo, M., Cervenka, J., and Luyten, F.P. (1996). A human chondrodysplasia due to a mutation in a TGF beta superfamily member. *Nat. Genet.* 12, 315–317.
- Thomas, J.T., Kilpatrick, M.W., Lin, K., Erlacher, L., Lembessis, P., Costa, T., Tsipouras, P., and Luyten, F.P. (1997). Disruption of human limb morphogenesis by a dominant negative mutation in CDMP1. *Nat. Genet.* 17, 58–64.
- Tickle, C. (1995). Vertebrate limb development. *Curr. Opin. Genet. Dev.* 5, 478–484.
- Wada, N., Kawakami, Y., Ladher, R., Francis-West, P.H., and Nohno, T. (1999). Involvement of Frzb-1 in mesenchymal condensation and cartilage differentiation in the chick limb bud. *Int. J. Dev. Biol.* 43, 495–500.
- Wolfman, N.M., Hattersley, G., Cox, K., Celeste, A.J., Nelson, R., Yamaji, N., Dube, J.L., DiBlasio-Smith, E., Nove, J., Song, J.J., et al. (1997). Ectopic induction of tendon and ligament in rats by growth and differentiation factors 5, 6, and 7, members of the TGF beta gene family. *J. Clin. Invest.* 100, 321–330.
- Wolpert, L. (1990). Signals in limb development: STOP, GO, STAY and POSITION. *J. Cell Sci. (Suppl 13)*, 199–208.
- Wright, E., Hargrave, M.R., Christiansen, J., Cooper, L., Kun, J., Evans, T., Gangadharan, U., Greenfield, A., and Koopman, P. (1995). The Sry related gene Sox9 is expressed during chondrogenesis in mouse embryos. *Nat. Genet.* 9, 15–20.
- Xu, L., Corcoran, R.B., Welsh, J.W., Pennica, D., and Levine, A.J. (2000). WISP 1 is a Wnt 1 and beta catenin responsive oncogene. *Genes Dev.* 14, 585–595.
- Yamaguchi, T.P., Bradley, A., McMahon, A.P., and Jones, S. (1999). A Wnt5a pathway underlies outgrowth of multiple structures in the vertebrate embryo. *Development* 126, 1211–1223.
- Zakany, J., and Duboule, D. (1993). Correlation of expression of Wnt-1 in developing limbs with abnormalities in growth and skeletal patterning. *Nature* 362, 546–549.
- Zakany, J., and Duboule, D. (1999). Hox genes in digit development and evolution. *Cell Tissue Res.* 296, 19–25.
- Zou, H., Wieser, R., Massague, J., and Niswander, L. (1997). Distinct roles of type I bone morphogenetic protein receptors in the formation and differentiation of cartilage. *Genes Dev.* 11, 2191–2203.